

## Transition Scenarios during the Evolution of the Belousov–Zhabotinsky Reaction in an Unstirred Batch Reactor

Mauro Rustici,\* Carlo Caravati, Enrico Petretto, Mario Branca, and Nadia Marchettini†

Università di Sassari, Dipartimento di Chimica, Via Vienna 2, 07100 Sassari, Italia

Received: January 22, 1999; In Final Form: May 19, 1999

We report experimental evidence of transition scenarios during the chemical evolution in an unstirred closed Belousov–Zhabotinsky (BZ) system. We demonstrate that during its chemical evolution the system spontaneously gives the following sequence of dynamic behavior before reaching equilibrium: period-1  $\rightarrow$  quasiperiodicity  $\rightarrow$  chaos  $\rightarrow$  quasiperiodicity  $\rightarrow$  period-1. Two transition scenarios are observed: at the onset of chaos and at its end. One appears as the mirror image of the other. Our observations support the view that closed chemical systems also are able to show chaotic behavior and the corresponding transition scenarios.

### I. Introduction

One of the major problems in nonlinear dynamics is discovering how the dynamic behavior of a system changes and evolves as its constraints (control parameters) are changed.<sup>1</sup> Nonlinear open chemical systems, for example, show various dynamic behaviors depending on the values of their control parameters. The Belousov–Zhabotinsky (BZ) reaction is widely known for its variety of dynamic regimes.<sup>2</sup> In continuous stirred tank reactor (CSTR) experiments, the parameters are the reagent concentrations and/or their residence times. The qualitative structure of the dynamics can change as parameters are varied. These qualitative changes are called bifurcations.

Complex and various dynamic behaviors have been experimentally observed and classified. Chaos is probably the most intriguing. Several means for the characterization of the chaotic behavior are available today. In particular, the individualization of the transition scenario leading to chaos supplements and supports the characterization of the chaotic state.

It is well established that closed chemical systems can exhibit various dynamic regimes. Nevertheless, these are strictly transient because closed systems naturally move through the parametric space. Indeed the parameters are not affected by any external action, but they spontaneously change during the chemical evolution until the ultimate equilibrium has been reached. However, transient behavior may be sustained for significant periods of time, and the chemical mixture can be considered to evolve in consecutive different pseudosteady states by spontaneous transitions. Therefore, with some special considerations, it is possible to study the dynamic states and the relative transition scenarios also for closed chemical systems. Evidently, particular attention must be paid to evaluate the stationarity of the signal. The successive transient states that spontaneously evolve during the chemical evolution seem to be risen through a bifurcation mechanism. Stryzhak and Pojman<sup>3</sup> presented evidence that in a semibatch reactor, where all phenomena are transient, it was possible to apply bifurcation analysis to explain the experimental results: the varying “initial

concentration” of a chemical in the vessel may be considered as a bifurcation parameter. According to that, the onset of these transitions between successive transient states can be then interpreted as a bifurcation.<sup>3</sup>

Not only simple oscillations but also chaotic behavior can take place in a closed BZ system. As a matter of fact, sensitivity to initial conditions has been pointed out in such systems at transient conditions both theoretically and experimentally.<sup>4–7</sup> Transient scenarios in the BZ system have also been the object of investigation.<sup>8–14</sup> For example, Wacker et al.<sup>15</sup> showed the existence of a transient spatiotemporal chaos for a reaction diffusion system. In 1980, Nagashima proved the existence of a chaotic state for the under nitrogen well stirred and temperature controlled batch BZ reaction.<sup>16</sup> Wang et al.<sup>17</sup> showed experimental evidence of successive transient period doubling and torus oscillations to transient chaos in a closed well mixed BZ system.

Our attention has been turned to the closed unstirred BZ system. Using suitable initial concentrations of reagents, this system shows various dynamic regimes despite the inevitable continuous drift toward the ultimate thermodynamic equilibrium. In particular, an aperiodic transient regime is followed by a periodic one. First, we proved the chaoticity of the aperiodic transient showing experimental evidence of the sensitivity of the system to its initial conditions, which is considered to be the major distinguishing feature of chaos.<sup>4</sup> Second, we also showed that the transition chaotic (aperiodic)  $\rightarrow$  periodic occurs via an inverse Ruelle–Takens–Newhouse (RTN) scenario.<sup>18</sup> The individuation of a typical scenario indirectly strengthened our characterization of the aperiodic transient as chaotic. It is important to note that a system shows the RTN scenario when, varying a system's parameter, the power spectrum will exhibit one, then two, and possibly three independent basic frequencies.<sup>19</sup> This type of behavior corresponds to the sequence period-1  $\rightarrow$  quasiperiodicity  $\rightarrow$  chaos, or, as far as the attractors in the phase space are concerned, limit cycle  $\rightarrow$  torus  $\rightarrow$  strange attractor.

In this paper we discuss how the chaos begins and the way it develops for an unstirred BZ system. We also discuss the complete sequence of regimes that appears during the chemical evolution of the reaction.

\* Corresponding author e-mail: rustici@ssmain.uniss.it.

† Università di Siena, Dipartimento di Scienze e Tecnologie Chimiche e dei Biosistemi, Pian dei Mantellini 44, 53100 Siena, Italia.

## II. Experimental Methods

All experiments were performed isothermally at room temperature ( $\sim 20^\circ\text{C}$ ) in a batch reactor (spectrophotometric cuvette,  $1 \times 1 \times 4 \text{ cm}^3$ ). The dynamics were monitored by the solution absorbance at 320 nm using quartz UV grade spectrophotometer cuvettes. A double beam spectrophotometer (Varian, series 634) was used. All chemicals were of analytical quality and were used without further purification. The following concentration of reactant's stock solutions were used:  $\text{Ce}(\text{SO}_4)_2$  0.004 M, malonic acid 0.30 M,  $\text{KBrO}_3$  0.09 M; each stock solution was 1 M  $\text{H}_2\text{SO}_4$ . The oscillator was started by mixing equal quantities of reactants in a flask and by stirring the solution for 10 min (with a Teflon-coated magnetic stirrer, length 1 cm) at a constant high stirring rate. The solution was then poured into the cuvette until the sample reached the top, and measurement of the signal began. The cross-sectional area of the spectrophotometer light beam was  $30 \text{ mm}^2$ . The volume spanned by the beam was  $300 \text{ mm}^3$  (7.5% of the total volume) and was located 2 cm away from the liquid-air interface, 1 cm away from the bottom of the cuvette and about 0.4 cm away from the sides.

Some experiments were performed by adding polyethylene-glycol ( $M_n = 3 \times 10^5$ ) during the chaotic phase of dynamics in order to modify viscosity of the medium and to obtain at least a preliminary evaluation of the importance of convection in affecting the dynamic behavior.

The spectrophotometer was connected to an IBM-compatible PC for data acquisition by an analogue to digital (board) converter with a 12 bit resolution. The absorbance was recorded with a  $\tau_s = 1 \text{ s}$  sampling time. Time series points were recorded and stored in a computer for data analysis.

## III. Results and Discussion

Figure 1a shows a spectrophotometric time series in which it is possible to note two transitions. We can represent this behavior by the following scheme: periodic  $\rightarrow$  aperiodic  $\rightarrow$  periodic. The aperiodic interval lasts for about 2 h. Our previous experiments<sup>4</sup> show that such behavior is an example of a chaotic transient. We think this is the right time to make a remark about the use of terms such as "periodic" used in this context. Strictly speaking, due to the transient nature of the system, the term periodic, for example, is not the most appropriate word to indicate the two nonaperiodic regions shown in Figure 1a. However, owing to the lack of commonly accepted terminology for some phenomena observed in batch reactors, we use terms such as "periodic" to indicate transient behavior of this kind (behavior whose power spectra show only one frequency when a sufficiently short time series fragment is considered, see later Figures 6a and 9c). The stirring effect on the dynamics of the system was also investigated.<sup>4</sup> No chaotic phase appears when stirring occurs, but only the periodic pattern is observed. The stirring effect will be more extensively discussed later.

To study the transition scenarios that occur in the absence of stirring, the spectral analysis, fast Fourier transform (FFT), was performed on sequential 1024 point portions of the time series. To increase the spectral resolution, we applied the zero filling technique. The short time fragments (1024 points) were transformed into longer time series sequences (2048 points) by adding a constant value equal to the minimum of the signal amplitude at the end of the fragments. In this way the spectral resolution  $\Delta f = 1/N \tau_s$ , where  $N$  is the number of points of the considered time fragment and  $\tau_s$  is the sampling time, was doubled. Discontinuities at the window edges have been reduced

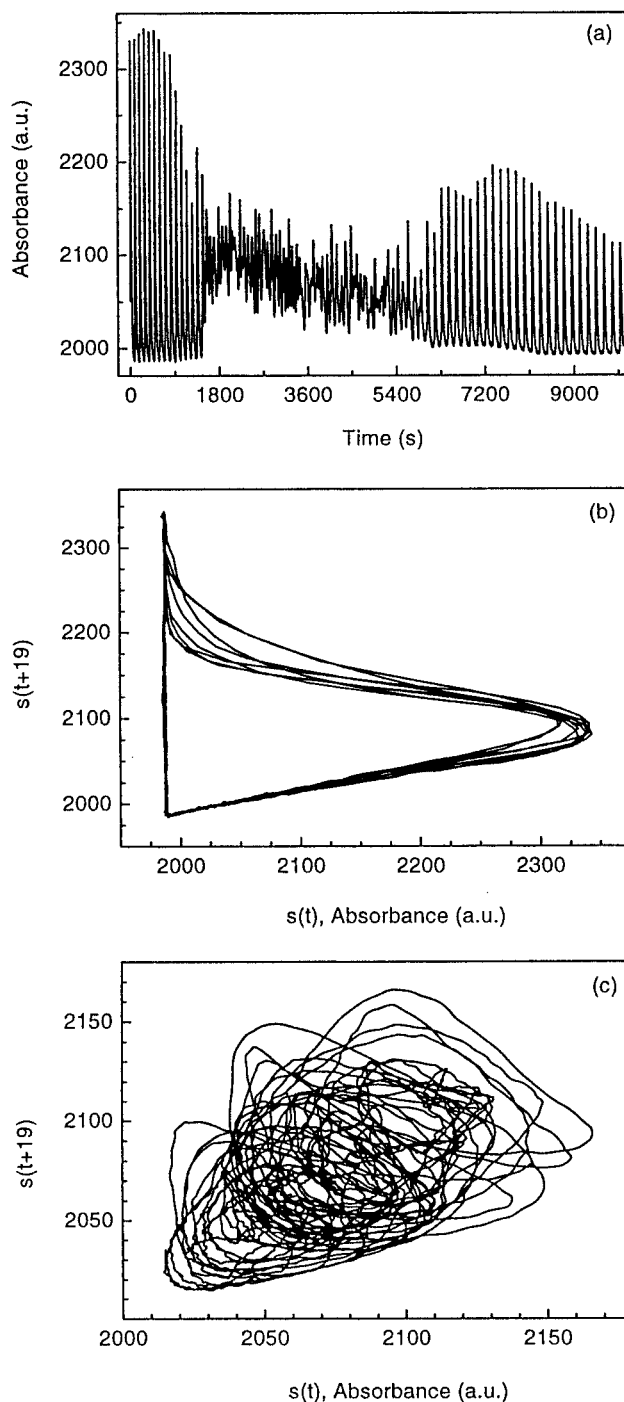


**Figure 1.** (a) Spectrophotometric recording ( $\lambda = 320 \text{ nm}$ , sampling time  $\tau_s = 1 \text{ s}$ ) at room temperature ( $\sim 20^\circ\text{C}$ ) in the absence of stirring. The time series exhibits two transitions: periodic  $\rightarrow$  aperiodic and aperiodic  $\rightarrow$  periodic. Three regions are thus observed: periodic, aperiodic, and periodic. (b) Projection of the reconstructed attractor (embedding dimension  $m = 10$ , time delay  $\tau = 19$ ) for the time series interval 1–1024 s on the plane  $(s_k, s_{k+\tau})$  is shown. (c) The same as (b) but for the 1800–5400 s time interval.

by multiplying the considered data with a Hanning window function.<sup>20</sup> This operation suppresses side lobes, which would otherwise be produced in the power spectrum of the signal.

As for other algorithms for the time series analysis, the FFT requires stationary data sets. Indeed, the lack of stationarity can raise distortions in the power spectrum. To check for the stationarity of time series portions, we preliminarily performed the recurrence plot calculation and the recurrence analysis.<sup>21–24</sup>

**A. Recurrence Analysis.** The whole considered experimental time series ( $s_1, s_2, \dots, s_n$ ),  $n = 14000$ , ( $s_j = s(t = j\tau_s)$  where  $\tau_s = 1$  s is the sampling time) quoted in Figure 1a was blocked into sequential  $N = 1024$  point long portions (epochs)

$$\begin{aligned} E_1 &= (s_1, s_2, \dots, s_N) \\ E_2 &= (s_{1+w}, s_{2+w}, \dots, s_{N+w}) \\ E_3 &= (s_{1+2w}, s_{2+2w}, \dots, s_{N+2w}) \\ &\vdots \\ E_p &= (s_{1+(p-1)w}, s_{2+(p-1)w}, \dots, s_{N+(p-1)w}) \end{aligned}$$

offset by  $w = 100$ . The number of epochs  $p$  is chosen in order to satisfy  $N + (p - 1)w \leq n$ . In this case a number of  $p = 130$  epochs resulted.

Sequential epochs were subjected to RQA. The RQA is an extension of the recurrence plot (RP). First introduced in a 1987 paper by Eckmann, Kamphorst, and Ruelle,<sup>21</sup> the RP is an analysis tool for experimental time series data. The RP is a graphical method designed to locate recurring patterns (hidden rhythms) and nonstationarities (drifts) in experimental data sets. To obtain the RP of each epoch  $E_i = (e_1, e_2, e_3, \dots, e_N) = (s_{1+(i-1)w}, s_{2+(i-1)w}, \dots, s_{N+(i-1)w})$ , the  $m$ -dimensional phase-space portrait of each time series epoch is reconstructed by the time delay method.<sup>25-27</sup> Thus, trajectories in the  $m$ -dimensional "embedding space" pass through the points

$$\begin{aligned} \mathbf{x}_1 &= \{e_1, e_{1+\tau}, e_{1+2\tau}, \dots, e_{1+(m-1)\tau}\} \\ \mathbf{x}_2 &= \{e_2, e_{2+\tau}, e_{2+2\tau}, \dots, e_{2+(m-1)\tau}\} \\ &\vdots \\ \mathbf{x}_q &= \{e_q, e_{q+\tau}, e_{q+2\tau}, \dots, e_{q+(m-1)\tau}\} \end{aligned}$$

where  $m$  is the embedding dimension,  $\tau$  is the time delay, and  $q$  satisfies  $q + (m - 1)\tau \leq N$ . Once the phase portrait for the considered epoch is reconstructed, a point  $\mathbf{x}_i$  is chosen on the trajectory and a ball of radius  $r$  centered on it;  $r$  is selected so that it contains a reasonable number of other points  $\mathbf{x}_j$  on the trajectory. The RP is constructed as an array of dots in a  $q \times q$  square, where a dot is drawn at  $(i, j)$  whenever  $\mathbf{x}_j$  is within the  $r$  radius ball (Euclidean distance) centered on  $\mathbf{x}_i$  (notice that, as  $\|\mathbf{x}_i - \mathbf{x}_j\| = \|\mathbf{x}_j - \mathbf{x}_i\|$ , the RP is symmetrical with respect to its main diagonal). Thus the RP is the plot of the recurrent points, where  $(i, j)$  is a recurrent point if the reconstructed vectors  $\mathbf{x}_i$  and  $\mathbf{x}_j$  are near each other (such as  $\|\mathbf{x}_i - \mathbf{x}_j\| \leq r$ ) in  $m$ -dimensional space. In this way the RP takes each single variable measurement time series epoch and projects it into multidimensional space by the embedding procedure identifying time correlations (recurrence) that are not apparent in the one-dimensional time series. However, RPs often contain subtle patterns that are not easily ascertained by qualitative visual inspection. The original visual description of RPs was improved by Webber et al.<sup>23</sup> by computing an array of specific recurrence variables that quantify the deterministic structure and complexity of the RPs. By plotting the recurrence variables as a function of the index of the very first point for each portion calculation, i.e., as a function of  $1 + jw$ ,  $j = 1, 2, \dots, p$ , it is possible to easily assess the quantitative features of the obtained sequential RPs. The recurrence analysis is far simpler and more objective than visual of the RP. Such an analysis constitutes the so-called RQA. This is very useful to evaluate the signal stationarity within each epoch and the possible transitions as the signal goes from epoch to epoch.

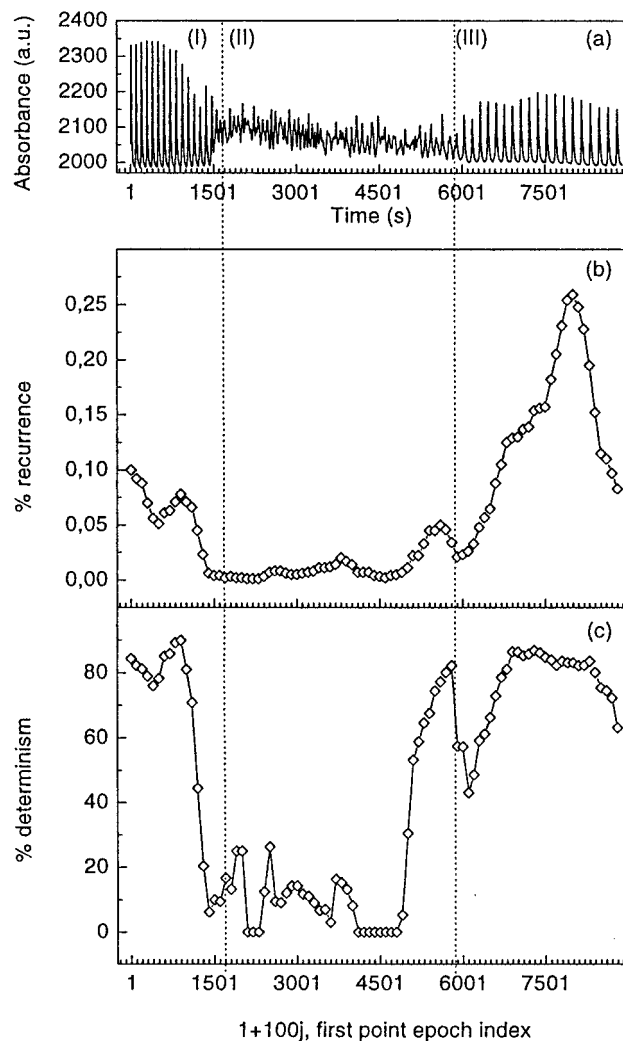


**Figure 2.** The spectrophotometric signal (a) was blocked off in sequential 1024-point epochs (1024 s). Each epoch of data was subjected to recurrence quantification analysis with embedding dimension  $m = 10$ , time delay  $\tau = 19$  and cutoff  $r = 4$  relative units (distances were scaled in order to get 100 as the mean distance). Here, % recurrence (b) and % determinism (c), epoch by epoch, were plotted as functions of the first point epoch index (i.e., as a function of time) with  $w = 100$  s increments. Therefore, the abscissae in (b) and (c) identify the very first point of each epoch analyzed.

For our aims we considered three recurrence variables: percent recurrence, percent determinism, and their ratio  $R$ .<sup>22,23</sup>

The % recurrence quantifies the percentage of the plot occupied by recurrent points. Thus, % recurrence =  $100(2q_r / (q^2 - q))$ , where  $q_r$  is the number of recurrent points upward the diagonal line. Periodic dynamics have higher percent recurrence values than aperiodic dynamics.

The % determinism quantifies the percentage of recurrent points that form upward diagonal line segments. Lines consist of two or more points that are diagonally adjacent with no intervening white space. Thus, % determinism =  $100(2q_l / (q^2 - q))$ , where  $q_l$  is the number of recurrent points that form upward diagonal line segments. This variable distinguishes recurrence points that are individually dispersed and those that are organized into specific diagonal patterns (deterministic dynamics repeat themselves, giving rise to diagonal line structure).

The ratio variable  $R$ , finally, is defined as the ratio of percent determinism to percent recurrence and addresses nonstationarity

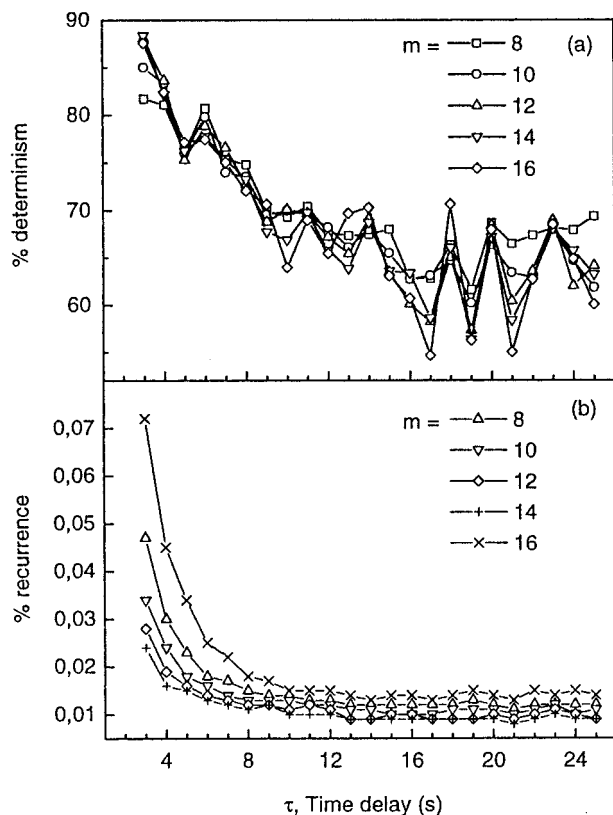


**Figure 3.** Here, % determinism (a) and % recurrence (b) are shown as a function of time delay  $\tau$  and embedding dimension  $m$  for the whole (II) aperiodic region (4906 points). A cutoff of  $r = 4$  relative units (mean distance = 100) was used.

characteristics in RP. In fact, during a transition, the percent recurrence usually decreases but the percent determinism is less affected; thus, the ratio value increases substantially but settles down again when a new quasi-steady state is achieved.

Figure 2 shows the % recurrence and determinism when the embedding dimension is 10 and the time delay is 19.<sup>24</sup> Each point quoted in Figure 2b,c refers to a recurrence analysis carried out on 1024 point portions. The abscissae identify the very first point for each portion calculation. A high % recurrence and determinism for the regions (I) and (III) can be seen as expected. On the contrary, the (II) region, corresponding to the aperiodic zone, displays a low % recurrence. The low percent determinism would seem to indicate a stochastic nature of the signal. Nevertheless, when the complete (II) region (4096 points) is considered, the % determinism increases, settling down to an acceptable value above 55%, (Figure 3a). On the other hand, the % recurrence remains very low ( $\leq 0.05\%$ ), (Figure 3b). The % determinism and % recurrence vanish when the signal is randomized.<sup>23</sup> These results demonstrate that the region (II) is a deterministic signal despite its aperiodic feature. This strengthens our previous findings,<sup>4</sup> namely that the aperiodic signal is nothing but a chaotic pattern.

The ratio variable  $R$  for the transition zones (a) periodic  $\rightarrow$  chaotic and (b) chaotic  $\rightarrow$  periodic is reported in Figure 4. In particular, Figure 4a allows us to locate the point  $\alpha$  up to which the signal can be considered pseudostationary. Similarly, in Figure 4b the point  $\beta$  was located after which the signal becomes pseudostationary and the regions pointed out in the dotted box and beyond the  $\beta$  point are pseudostationary.

The spectral analysis of portion data requires that the signal within each portion be stationary, as previously mentioned. The

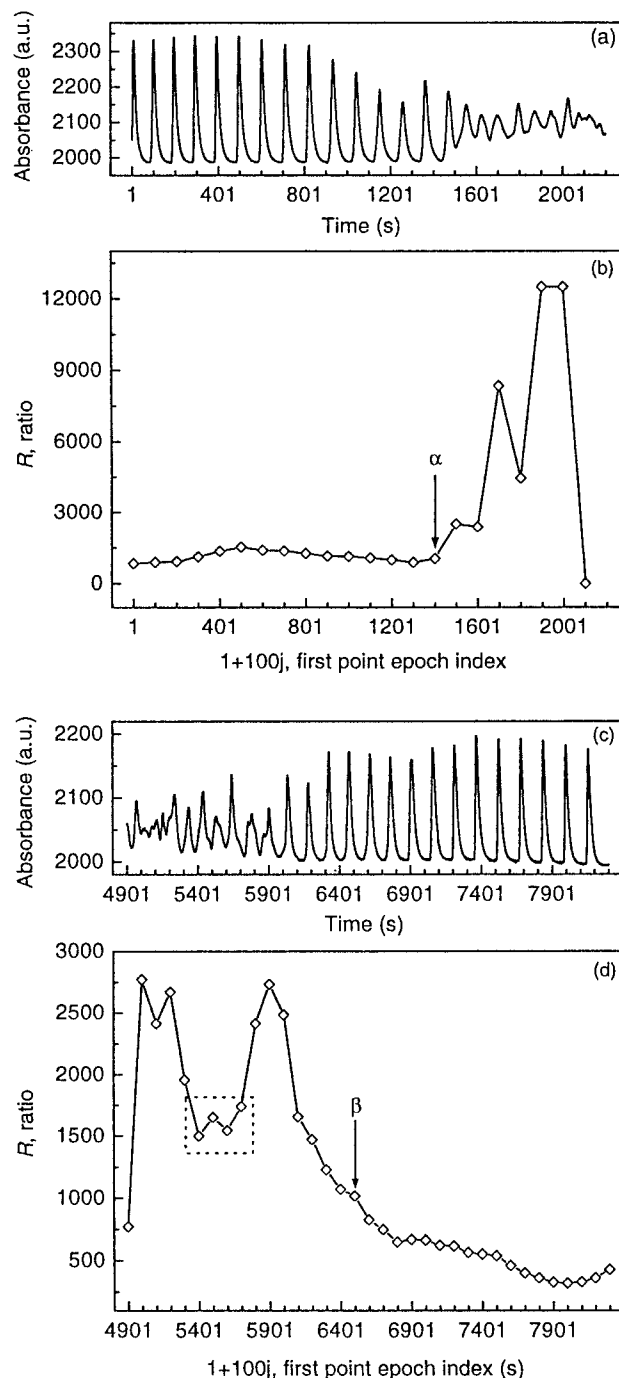


**Figure 4.** Ratio variable values, (b) and (d), respectively, pertaining to the first (a) and second (c) transition zones as a function of the first point epoch index (epochs are offset by  $w = 100$ ). Parameter settings:  $m = 10$ ,  $\tau = 19$ ,  $r = 4$  relative units (mean distance = 100). Before the point  $\alpha$  after the point  $\beta$  and within the dotted box the signal can be considered stationary.

previous discussion on Figure 4 suggest that short 1024 point portions starting within time intervals 1–1400 s, 5400–5700 s, and 6400–8400 s are stationary. Therefore, it is possible to apply the FFT algorithm to 1024 point portions starting within the above-mentioned time intervals.

**B. Time Series and Power Spectra Analysis. First Transition: Periodic  $\rightarrow$  Chaotic.** Three regions isolated from Figure 1a are reported in Figure 5. Notice that the regions (a) and (b) belong to the stationary time intervals previously individuated. The power spectra of the regions (a), (b), and (c) are shown in Figure 6.

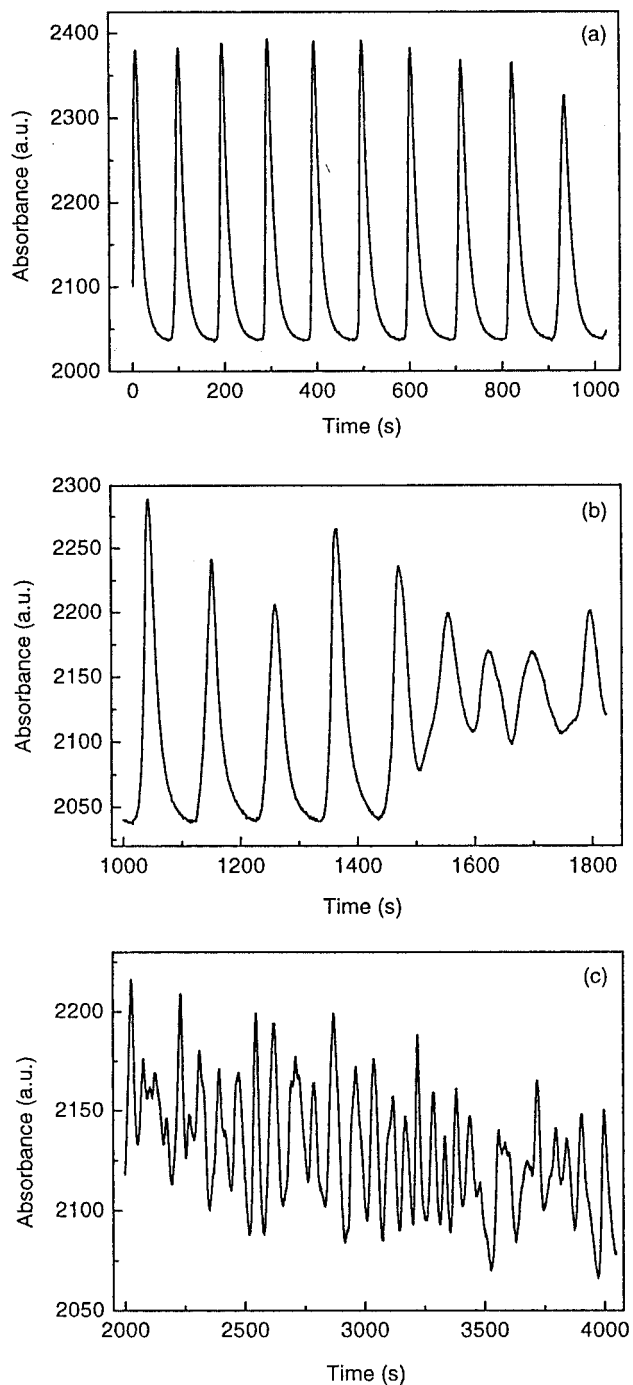


**Figure 5.** First transition: periodic  $\rightarrow$  chaotic. Three different regions isolated from the time series of Figure 1a are shown: (a) periodic region, (b) intermediate region, (c) aperiodic region.

As illustrated in Figure 6a, the starting periodic regime is nearly sinusoidal with only a few harmonics of the fundamental frequency ( $f_1 \sim 0.01$  Hz) above the noise level.

After about 15 min, we can point out (Figure 6b) the appearance of a new frequency ( $f_2 \sim 0.007$  Hz) smaller than  $f_1$ . The combination frequencies  $|af_1 + bf_2|$ , where  $a$  and  $b$  are small integers, are also observed. The birth of the new frequency  $f_2$  and one of the combinations with  $f_1$  during the chemical evolution is reported in Figure 7. A quasiperiodic regime takes place.

After an additional 15 min, the FFT of the aperiodic region gives a broadband spectrum, Figure 6c.

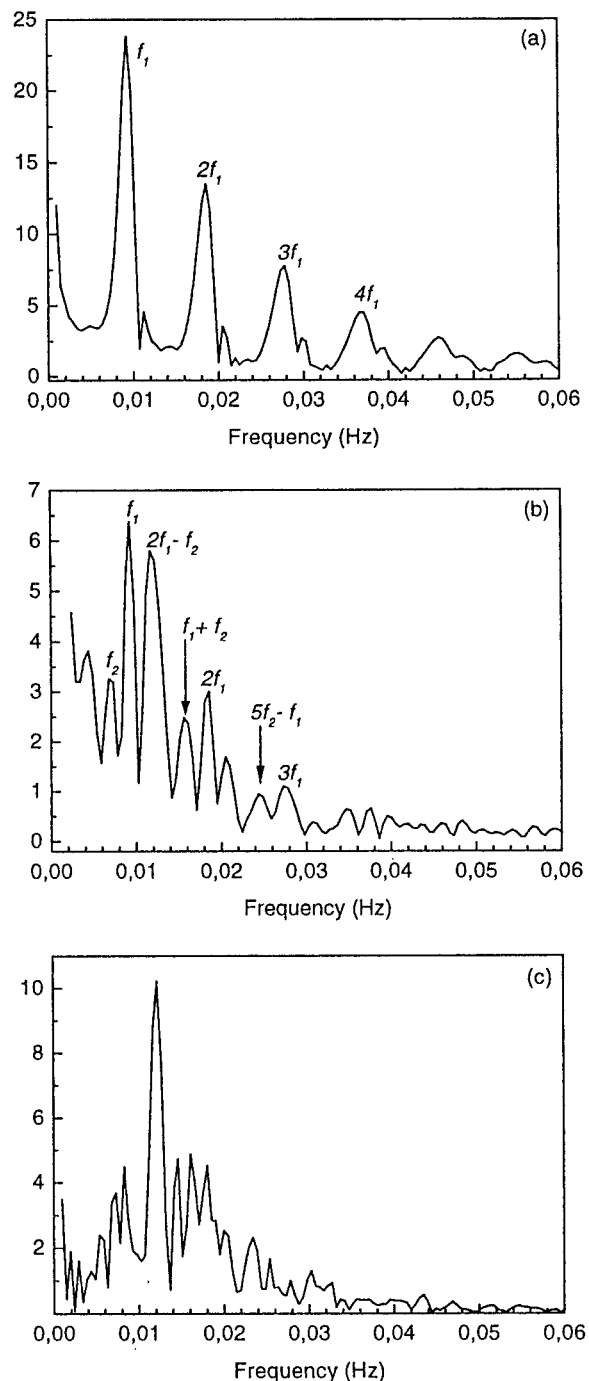


**Figure 6.** Here, (a), (b), and (c) show the square of the Fourier transform of the time series of Figure 5a, b, c, respectively. Notice, in (b), the existence of two frequencies not rationally related.

The chaotic quality of the aperiodic region being already proved,<sup>4</sup> the sequence periodic (limit cycle)  $\rightarrow$  quasiperiodic (torus)  $\rightarrow$  chaotic (strange attractor) can be identified by inspection of Figure 6. This proves the occurrence of the RTN scenario. This is the first time that a transient RTN scenario has been observed during the temporal evolution of an unstirred closed BZ system.

It is interesting to hypothesize in which way such a scenario takes place. Previous findings proved that the interplay between chemical kinetics and diffusion-convective processes is of paramount importance for the appearance of the chaotic phase. Indeed, the system does not show any chaotic phase when stirring occurs.<sup>4</sup> We take note that diffusion and convection

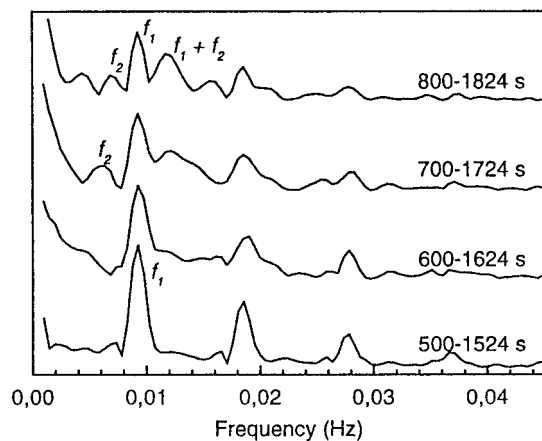


**Figure 7.** Square of the Fourier transform of sequential time series portions shifted by 100 points (100 s) corresponding to the transition region. The time interval 500–1824 s is considered. Notice the gradual rising of the frequency  $f_2$  and the appearance of the combination band  $f_1 + f_2$ .

spontaneously occur in the absence of stirring. The first transition (Figure 1a) takes place in a short period (about 25 min). Moreover, when the stirring was started only after the aperiodic behavior occurred, periodic oscillations suddenly appeared; on the other hand, some time (about 8 min) is required to recover the aperiodic pattern after the stirring is stopped.<sup>4</sup> In these lapses of time, the convective and diffusive processes develop, while the concentration of the reactants remains practically unchanged. Then the chaotic behavior observed, which appears under nonstirring condition, begins as soon as the diffusion and convective processes occur. Therefore, the coupling of the chemical reaction rate with diffusion and convection should govern the quasiperiodic and chaotic spatiotemporal evolution. In this work, we do not provide any mechanistic interpretation of the transition scenario observed: nevertheless, we suggest that diffusive and convective motions appear to be good candidates to understand the bifurcation mechanism underlying the observed transition scenario.

To evaluate the role that the convection plays in determining the dynamic behavior of the system, we tried to eliminate convective motions. A sure way to reach this goal was to run the reaction in a gel medium.<sup>28</sup> Nevertheless, some chemicals (for example polyethylene glycol) are able to increase the medium viscosity, thus reducing the convective motions. Taking advantage of this, we added to the reaction solution polyethylene glycol (0.50 mg/mL). We observed the disappearance of the chaotic phase: only periodic behavior occurred. We conclude that convection plays a critical role in this first transition scenario. Nevertheless, the convection could be buoyancy-driven or surface-tension-driven. To distinguish which type of convections couple to local kinetics, we performed the experiment with a cuvette completely filled and sealed. In this way we eliminated the air/water interface and consequently the surface-tension-driven convection. No significant difference in the dynamic behavior was observed. Thus, the convection that is coupled to kinetics is believed to be buoyancy driven.

We suggest that the dynamic behavior of this system should be modeled by reaction–diffusion–convection equations, where the convection effects would occupy the crucial role in describing the observed RTN transition scenario. The recently proposed Legawiec and Kawczyński model,<sup>29</sup> suitable when completed in order to take into account the buoyancy-driven convection,<sup>30</sup> could be a good starting point to interpret our experimental results.

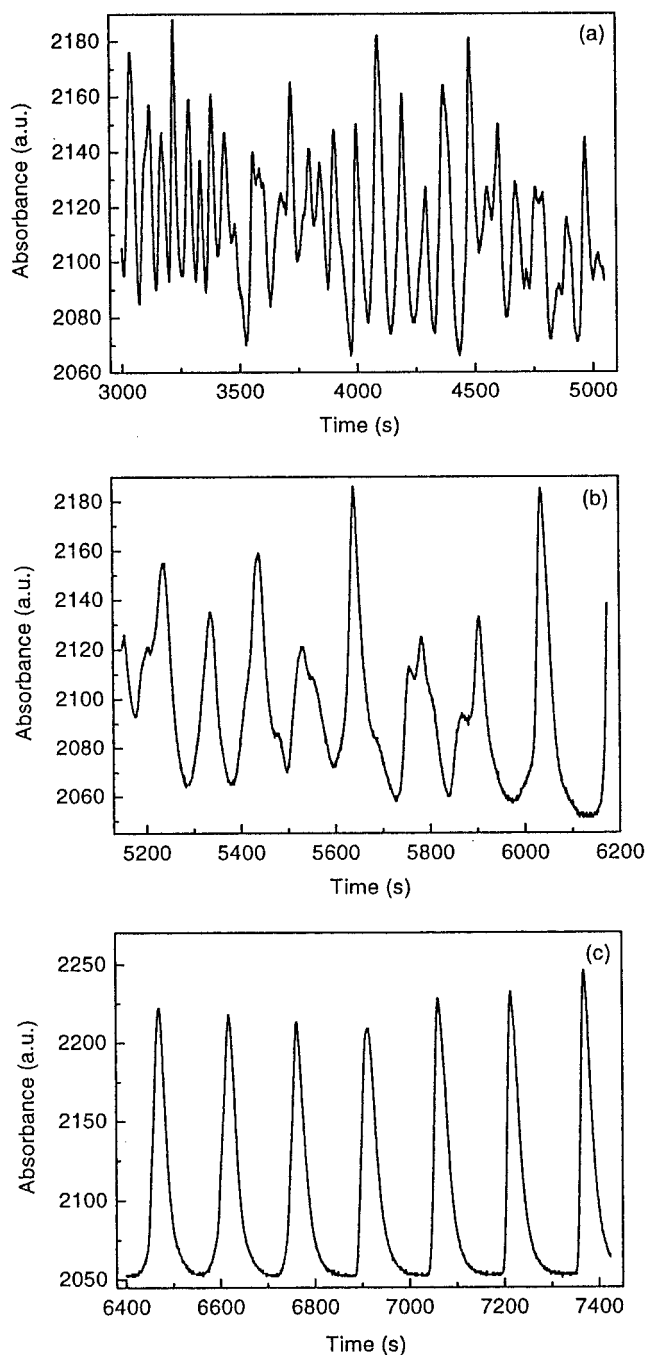


**Figure 8.** Second transition: chaotic  $\rightarrow$  periodic. Three different time intervals of the run quoted in Figure 1a are shown: (a) chaotic zone, (b) transition zone, and (c) periodic zone.

*Second Transition: Chaotic  $\rightarrow$  Periodic.* Figure 8a shows the last portion of the chaotic region before the appearance of the new periodic interval (Figure 8c). The intermediate region is shown on Figure 8b. The FFTs of the temporal series belonging to these three regions are shown on Figure 9. Figure 9a shows the typical broadband spectrum characteristic either of noise or chaotic signals. The power spectra shown in Figure 9c display the fundamental frequency ( $f_1 \sim 0.006$  Hz) and a few harmonics. The power spectrum of the intermediate region (Figure 9b) shows the existence of two frequencies ( $f_2 \sim 0.005$  and  $f_1 \sim 0.008$  Hz) and their combinations which are not rationally related. The power spectra displayed in Figure 9 correspond to the following bifurcation scheme: chaos  $\rightarrow$  quasiperiodicity  $\rightarrow$  period-1. The appearance of this behavior

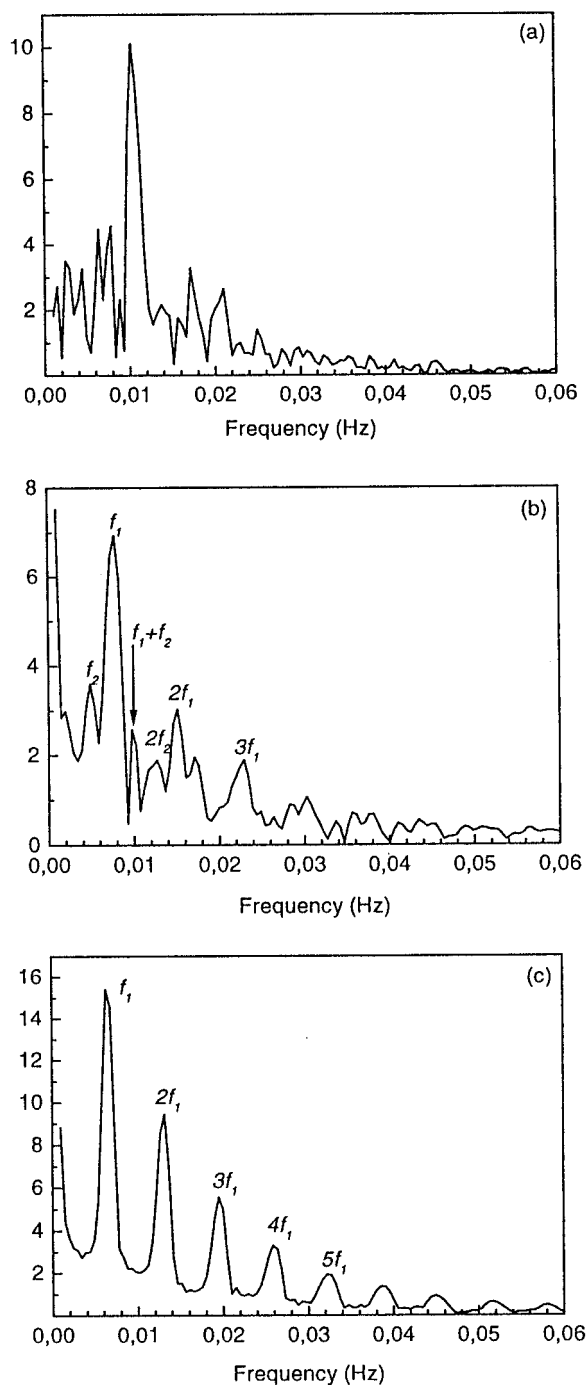


**Figure 9.** Here, (a), (b), and (c) show the square of the Fourier transform of the time series of Figure 8a, b, c, respectively. Notice, in (b), the existence of two frequencies not rationally related.

should be a manifestation of an inverse RTN scenario; this result gives added weight to our previous work.<sup>18</sup>

It is interesting to note that chaotic behavior starts by an RTN scenario and ends by an inverse RTN scenario. Nevertheless, we suggest that for the inverse RTN transition (chaos  $\rightarrow$  periodicity), the bifurcation parameter should not be the same as the one that we hypothesized could cause the RTN transition (periodicity  $\rightarrow$  chaos). It is reasonable to suppose that after the onset of the chaotic phase, the diffusion and convection

properties do not change any further. In this lapse of time (about 2 h) a strong consumption of reactants occurred. The reactant concentrations seem to be responsible for the second transition chaos  $\rightarrow$  quasiperiodicity  $\rightarrow$  period-1.

#### IV. Conclusions

The results presented above give further evidence that the aperiodic behavior observed in an unstirred batch BZ reaction is an example of transient spatiotemporal chaos. We have also demonstrated for the first time the chaotic behavior arising in an RTN scenario and dying out by an inverse RTN scenario. One scenario appears as the mirror image of the other. Nevertheless, such symmetry does not seem to involve the bifurcation parameters. The onset of chaos occurs by the interplay of local kinetics, diffusion and convection. The end of chaos is related to the consumption of the reactants.

Such results demonstrate once more that closed chemical systems are capable of displaying chaos even in the presence of the inevitable effects of reactant consumption.

**Acknowledgment.** We thank J. Pojman for helpful discussions. This work has been supported by COFIN.MURST97 CFSIB.

#### References and Notes

- (1) Nicolis, G. *Introduction to nonlinear science*; (Cambridge University Press: Cambridge, 1995).
- (2) Scott, S. K. *Chemical chaos*; Oxford University Press: Oxford, 1991.
- (3) Strizhak, P. E.; Pojman, J. A. *Chaos* **1996**, *6*, 461.
- (4) Rustici, M.; Branca, M.; Caravati, C.; Marchettini, N. *Chem. Phys. Lett.* **1996**, *263*, 429.
- (5) Scott, S. K.; Peng, B.; Tomlin, A. S.; Showalter, K. J. *Chem. Phys.* **1991**, *94*, 1134.
- (6) Johnson, B. R.; Scott, S. K.; Thompson, B. W. *Chaos*, **1997**, *7*, 350.
- (7) Coveney, P. V.; Chaudry, A. N. *J. Chem. Phys.* **1992**, *97*, 7448.
- (8) Salter, L. F.; Sheppard, J. G. *Int. J. Chem. Kinet.* **1982**, *14*, 815.
- (9) Ruoff, P.; Noyes, R. M. *J. Phys. Chem.* **1985**, *89*, 1339.
- (10) Kawahito, J.; Fujieda, S. *Thermochim. Acta* **1992**, *210*, 1.
- (11) Yatsimirskiy, K. B.; Strizhak, P. E. *Theor. Eksper. Chem.* **1992**, *28*, 382.
- (12) Strizhak, P. E.; Ivashchenko, T. S.; Yatsimirskiy, K. B. *Dokl. Acad. Sci. USSR* **1992**, *322*, 107.
- (13) Strizhak, P. E.; Ivashchenko, T. S.; Kawczyński, A. L. *Polish J. Chem.* **1994**, *68*, 2049.
- (14) Strizhak, P. E.; Kawczyński, A. L. *J. Phys. Chem.* **1995**, *99*, 10830.
- (15) Wacker, A.; Bose, S.; Schöll, E. *Europhys. Lett.* **1995**, *31*, 257.
- (16) Nagashima, H. *J. Phys. Soc. Jpn.* **1980**, *49*, 681.
- (17) Wang, J.; Sorensen, P. G.; Hynne, F. *J. Phys. Chem.* **1994**, *98*, 725.
- (18) Rustici, M.; Branca, M.; Brunetti, A.; Caravati, C.; Marchettini, N. *Chem. Phys. Lett.* **1998**, *293*, 145.
- (19) Eckmann, J. P. *Rev. Mod. Phys.* **1981**, *53*, 643.
- (20) Kay, S. M.; Marple, S. L. *Proc. IEEE* **1981**, *69*, 1380–1419.
- (21) Eckmann, J. P.; Kamphorst, S. O.; Ruelle, D. *Europhys. Lett.* **1987**, *4*, 973.
- (22) Zbilut J. P.; Webber, C. L., Jr. *Phys. Lett. A* **1992**, *171*, 199.
- (23) Webber, C. L., Jr.; Zbilut, J. P. *J. Appl. Physiol.* **1994**, *76*, 965.
- (24) Iwanski, J. S.; Bradley, E. *Chaos* **1998**, *8*, 861.
- (25) Takens, F. In *Lecture Notes in Mathematics*; Rand, D. A., Young, L. S., Eds.; Springer: Berlin, 1981; Vol. 898, p 366.
- (26) Eckmann J. P.; Ruelle D. *Rev. Mod. Phys.* **1985**, *57*, 617.
- (27) Abarbanel, H. D. I.; Brown, R.; Sidorowich, J. J.; Tsimring, L. S. *Rev. Mod. Phys.* **1993**, *64*, 1331.
- (28) Pojman J. A.; Epstein, I. *J. Phys. Chem.* **1990**, *94*, 4966.
- (29) Legawiec, B.; Kawczyński, A. L. *J. Phys. Chem.* **1997**, *101*, 8063.
- (30) Turner, J. S. *Buoyancy effects in fluids*; Cambridge University Press: Cambridge, 1973.